

Social contagions with communication channels alternation on multiplex networks

Wei Wang^{1,2,3}, Ming Tang^{2,3,4}, H. Eugene Stanley⁵, Lidia A. Braunstein^{5,6}

¹ College of Computer Science and Technology, Chongqing University of Posts and Telecommunications, Chongqing 400065, China

² Web Sciences Center, University of Electronic Science and Technology of China, Chengdu 610054, China

³ Big Data Research Center, University of Electronic Science and Technology of China, Chengdu 610054, China

⁴ School of Information Science and Technology, East China Normal University, Shanghai, 200241, China

⁵ Center for Polymer Studies and Department of Physics, Boston University, Boston, Massachusetts 02215, USA

⁶ Instituto de Investigaciones Físicas de Mar del Plata (IFIMAR)-Departamento de Física, Facultad de Ciencias Exactas y Naturales, Universidad Nacional de Mar del Plata-CONICET, Funes 3350, (7600) Mar del Plata, Argentina

E-mail: wwzqbx@hotmail.com; tangminghan007@gmail.com

Abstract. Internet communication channels, e.g., Facebook, Twitter, and email, are multiplex networks that facilitate interaction and information-sharing among individuals. During brief time periods users often use a single communication channel, and communication channel alteration (CCA) occurs, which means that our understanding of the dynamics of social contagions must be redefined. We propose a non-Markovian behavior spreading model that takes into account the CCA mechanism in multiplex networks, and we develop a generalized edge-based compartmental theory to describe the spreading dynamics. Through extensive numerical simulations and theoretical analyses, we find that the time-delays induced by the CCA characteristic slows the behavior spreading but does not affect the final adoption size. We also find that the CCA characteristic suppresses behavior spreading and that the information transmission probability in ER-SF multiplex networks introduces a crossover in adoption size from continuous to discontinuous behavior. Our results extend our understanding of the role of the CCA characteristic in spreading dynamics, and may elicit further research.

PACS numbers: 89.75.Hc, 87.19.X-, 87.23.Ge

Contents

1 Introduction 2

2 Social contagion model on multiplex networks 3

3 Theory 5

4 Numerical simulations 11

4.1 RR-RR multiplex networks 11

4.2 ER-SF multiplex networks 13

5 Conclusions 15

1. Introduction

There are numerous social communication platforms, e.g., Facebook, Twitter, and email, that participate in the current world-wide information explosion. These platforms taken together behave as a network of networks (NON) in which each communication platform functions as a subnetwork [1, 2, 3, 4]. These NONs can be multilayer, interdependent, or multiplex. In interdependent networks the functionality of the components in one network depends on the functionality of nodes in other networks. A multiplex network is a special NON case in which each agent can be present in more than one layer. Extensive studies of cascading failure, evolutionary games, synchronization, and spreading dynamics have found that the dynamics on NONs differ greatly from those on single networks [5, 6, 7, 8, 9, 10, 11]. For example, Buldyrev *et al.* found a first-order percolation phase transition in interdependent networks that is qualitatively different from the second-order phase transition in single networks [7].

Spreading dynamics in complex networks can be classified as either biological or social contagions. In biological contagions such as epidemic spreading, researchers have found that multilayer networks promote spreading [9, 8], induce the coexistence of mixed phase transitions [12], and produce rare-region phenomena [13]. In contrast to biological contagions, social contagions are strongly affected by social reinforcement [14]. Research on social contagions has focused primarily on a generalized Watts threshold model [15, 16, 17, 18, 19, 20]. As in biological contagions, the behavior of NONs promotes social contagions [15]. Majdandzic *et al.* found multiple tipping points in multilayer networks [20, 21]. Recently Wang *et al.* used a data-driven asymmetrical social-biology coevolution model to locate an optimal information diffusion mechanism for suppressing biological contagions [22] that enables us to understand the effect of asymmetry in interacting dynamics [23, 24, 25, 26].

When we face with various kinds of communication channels, we usually choose only one to transmit information to friends during a short period due to inelastic resources (e.g., time and energy) [27, 28, 29]. As a result, when transmitting information through a multiplex network we often migrate to other channels [30, 31] and a communication channel alteration (CCA) characteristic occurs. For instance, we transmit an information to our friends by short

message or email, thus we only active in short message network or email network. When the CCA characteristic is introduced, we know (i) delays in an individual's ability to obtain information from other platforms and (ii) a memory effect to occur when the information is finally obtained. Theoretically CCA characteristic induces a non-Markovian effect into the spreading dynamics that further causes strong dynamic correlations among the states of neighbors.

Because there has been no systematic study of how CCA characteristic affects the dynamics of social contagions on multiplex networks, we propose a non-Markovian behavior spreading model on multiplex networks. At any given time an individual can be active in only one communication layer, and can transmit behavioral information to neighbors and obtain behavioral information from neighbors within the same subnetwork. Through extensive numerical simulations we find that the time delays induced by CCA characteristic slow the behavior spreading but do not affect the final adoption size. We also find that CCA characteristic suppresses behavior spreading, and that the final size of the adoption versus the behavioral information transmission probability changes from continuous (discontinuous) to discontinuous (continuous) in ER-SF networks. We develop a generalized edge-based compartmental theory to describe this non-Markovian spreading model, and find that the theoretical predictions agree with the numerical predictions.

2. Social contagion model on multiplex networks

Such communication channels as Facebook, Twitter, and Email facilitate interaction and information-sharing. Taken together they form a multiplex network in which each communication channel functions as a subnetwork. During short periods of time individuals select a single communication platform to transmit information, and then a CCA characteristic emerges. To understand how the CCA characteristic affects the dynamics of social contagion, we examine the behavior spreading dynamics in two-layer multiplex networks in which each layer or subnetwork represents a single communication channel. Figure 1(a) shows a multiplex network. In the multiplex network model, subnetworks \mathcal{A} and \mathcal{B} have the same number of nodes, and they randomly match one-to-one, which means that each individual can communicate with friends through two different communication channels. To establish the multiplex network we first assign degrees $k_{\mathcal{A}}$ and $k_{\mathcal{B}}$ to individuals in subnetworks \mathcal{A} and \mathcal{B} , respectively, according to a joint degree distribution $P(\vec{K}) = P(k_{\mathcal{A}}, k_{\mathcal{B}})$. We then build each subnetwork using an uncorrelated configuration model [32]. In the thermodynamic limit, i.e., the network size $N \rightarrow \infty$, there are no intra-layer degree correlations in the subnetworks.

We propose a generalized non-Markovian susceptible-adopted-recovered (SAR) model [33, 34, 35] to describe the behavior spreading dynamics in multiplex networks. In the SAR model, social reinforcement is triggered by the reception of non-redundant behavioral information, i.e., a susceptible individual adopts the new behavior only when the amount of received non-redundant information from neighbors rises above a given adoption threshold. Non-redundant information means that repetitive information transmission on every edge is forbidden. An individual in the susceptible state has not adopted the behavior. An individual

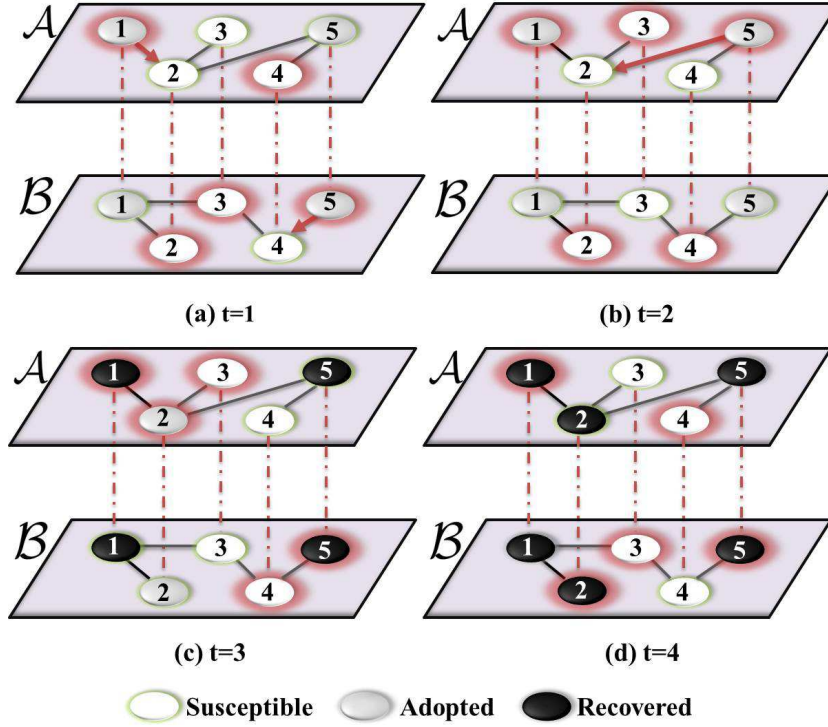


Figure 1. (Color online) Illustration of social contagions on multiplex networks. Initially, individuals 1 and 5 are selected as seeds (adopted), and the remaining individuals are susceptible. (a) At time $t = 1$, individual 1 (5) successfully transmits the information to his susceptible neighbor 2 (4) in subnetwork \mathcal{A} (\mathcal{B}). The accumulated pieces of information of 2 (4) in subnetwork network \mathcal{A} (\mathcal{B}) is $m_2^{\mathcal{A}} = 1$ ($m_4^{\mathcal{B}} = 1$). (b) At time $t = 2$, individuals 1, 3 and 5 are in subnetwork \mathcal{A} . Individual 5 successfully transmits the information to 2, however, individual 2 does not read know this information since he belongs to subnetwork \mathcal{B} . (c) At $t = 3$, individual 2 activates in subnetwork \mathcal{A} , he opens his inbox and fulfills his adoption threshold $T_{\mathcal{A}} = 2$. Thus, individual 2 adopts the behavior. Individuals 1 and 5 recover with probability $\gamma = 0.6$. (d) At time $t = 4$, all adopted individuals recover and no individual whose received information is greater than his adoption threshold. The processes terminates. Each individual activates in subnetwork \mathcal{A} with probability $p = 0.6$, and in subnetwork \mathcal{B} with the complementary probability $1 - p = 0.4$. Individuals activates in the subnetwork are marked with red shadow, such as individual 1 activates in \mathcal{A} .

in the adopted state has adopted the behavior and is willing to transmit the information to neighbors through one communication channel. An individual in the recovered state has lost interest in the behavior and no longer spreads the information.

During short periods of time the constraints posed by inelastic resources limit individuals to a single communication channel [36, 37], i.e., at any given time step an individual can only be active in one subnetwork. Individuals thus exhibit a communication channels alternation (CCA) during the time evolution. To describe this CCA characteristic, we introduce a layer-switching parameter p_i and assume that individual i is active in subnetwork \mathcal{A} with a probability p_i and active in subnetwork \mathcal{B} with a probability $1 - p_i$. When an individual is active in a subnetwork $\mathcal{X} \in \{\mathcal{A}, \mathcal{B}\}$, they can transmit the information to neighbors in

subnetwork \mathcal{X} and can only read information from neighbors in subnetwork \mathcal{X} but cannot read the information in the other non-active subnetwork \mathcal{Y} . Thus individuals cannot simultaneously read all the information from all neighbors in all communication channels, and this introduces *time-delays* in information reading.

We use a synchronous updating method [38] to renew the states of individuals. We first randomly select a fraction ρ_0 of individuals as seeds in the adopted state. The remaining individuals are in the susceptible state. At each time step, each adopted individual $v_{\mathcal{X}}$ active in subnetwork \mathcal{X} transmits the information to each susceptible neighbor $u_{\mathcal{X}}$ with a probability $\lambda_{\mathcal{X}}$. When individual $v_{\mathcal{X}}$ successfully transmits information to $u_{\mathcal{X}}$, the information transmission between them does not occur in subsequent steps, i.e., we only allow nonredundant information transmission between two individuals because each neighbor can only partially guarantee the credibility and legitimacy of the behavior [39]. Note that if a susceptible individual $u_{\mathcal{X}}$ is active in subnetwork \mathcal{X} , they only have read information in subnetwork \mathcal{X} . If an individual $u_{\mathcal{X}}$ in subnetwork \mathcal{X} receives a new piece of information, he will adopt the behavior with a probability $\pi(m_u^{\mathcal{A}}, m_u^{\mathcal{B}})$, where the $m_u^{\mathcal{X}}$ value is the number of cumulative pieces of nonredundant information from neighbors in subnetwork \mathcal{X} . If individual $u_{\mathcal{X}}$ adopts the behavior, his counterpart $u_{\mathcal{Y}}$ also becomes adopted in subnetwork \mathcal{Y} . Here we focus on a specific case in which an individual in the susceptible state adopts the new behavior when $m_u^{\mathcal{X}}$ exceeds their adoption threshold $T_u^{\mathcal{X}}$ in subnetwork \mathcal{X} . For simplicity, we assume all individuals have the same adoption threshold $T_u^{\mathcal{X}} = T_{\mathcal{X}}$ in subnetwork \mathcal{X} . The $\pi(m_u^{\mathcal{A}}, m_u^{\mathcal{B}})$ value is

$$\pi(m_u^{\mathcal{A}}, m_u^{\mathcal{B}}) = \begin{cases} 1, & m_u^{\mathcal{A}} \geq T_{\mathcal{A}} \text{ or } m_u^{\mathcal{B}} \geq T_{\mathcal{B}}, \\ 0, & \text{others.} \end{cases} \quad (1)$$

To include the social reinforcement effect, both $T_{\mathcal{A}}$ and $T_{\mathcal{B}}$ values are greater than unity. At each time step we assume that all individuals in the adopted state lose interest in transmitting the information and with a probability γ they recover. The spreading stops when all the adopted individuals become recovered and the received information of all the susceptible individuals is not greater than their threshold in either subnetwork. Figure 1 shows the behavior spreading dynamics on multiplex networks.

3. Theory

From the description of the behavior adoption process in Sec. 2 we know that there is a *non-Markovian* characteristic in the dynamics because (i) social reinforcement occurs when non-redundant behavioral information transmissions are remembered, and (ii) the CCA characteristic causes time-delays in reading information. This non-Markovian characteristic makes the strong dynamic correlations among the states of the neighbors difficult to describe. Here we develop a generalized edge-based compartmental theory [40, 41, 42, 43] to describe the spreading of behavior in multiplex networks.

An individual u adopting the new behavior must take into account their received information in both subnetworks \mathcal{A} and \mathcal{B} . Denoting $u_{\mathcal{X}}$ as an individual u active in

subnetwork $\mathcal{X} \in \{\mathcal{A}, \mathcal{B}\}$, we quantify the probability that individual u is in the susceptible state and assume that $u_{\mathcal{X}}$ is in the cavity state [44], i.e., that $u_{\mathcal{X}}$ cannot transmit the information to neighbors in subnetwork \mathcal{X} but can receive information from neighbors in all subnetworks. The probability that an individual $v_{\mathcal{X}}$ has not transmitted the information to a neighbor $u_{\mathcal{X}}$ along a randomly chosen edge in subnetwork \mathcal{X} by time t is $\theta_{\mathcal{X}}(t)$. At time t , the probability that $u_{\mathcal{X}}$ has received units of information $m_{\mathcal{X}}$ from subnetwork \mathcal{X} is

$$\phi_{m_{\mathcal{X}}}^{\mathcal{X}}(k_{\mathcal{X}}, t) = \binom{k_{\mathcal{X}}}{m_{\mathcal{X}}} [\theta_{\mathcal{X}}(t)]^{k_{\mathcal{X}} - m_{\mathcal{X}}} [1 - \theta_{\mathcal{X}}(t)]^{m_{\mathcal{X}}}, \quad (2)$$

where $k_{\mathcal{X}}$ is the degree of individual u in subnetwork \mathcal{X} . Here the CCA characteristic disallows individual $u_{\mathcal{X}}$ from quickly reading all the information they have received in all subnetworks since an individual can read all the information from the layer in which they are currently active. At time t , an individual u can read all the information from neighbors in subnetwork \mathcal{X} if he is active in this subnetwork. If he is active in the corresponding subnetwork \mathcal{Y} , he can read the information received at only the most recent time that he is active in subnetwork \mathcal{X} .

Because this process is stochastic [45], the time interval between two successive active states in the same subnetwork \mathcal{A} is $P_{\mathcal{A}}(\bar{\omega}) \sim e^{-(1-p_u^{\mathcal{A}})\bar{\omega}}$ and the average interval time is $1/(1-p_u^{\mathcal{A}})$, where $p_u^{\mathcal{A}}$ is the probability that u is active in subnetwork \mathcal{A} [see Figs. 2(a)–(b) and (d)–(e)]. Thus the average time interval of an individual active in subnetwork \mathcal{X} is

$$\varpi_{\mathcal{X}} = \frac{1}{N} \sum_{u=1}^N \frac{1}{1-p_u^{\mathcal{X}}}. \quad (3)$$

Thus when individual u is active in subnetwork \mathcal{Y} , they can only read information in the inbox of subnetwork \mathcal{X} up to time $t - \varpi_{\mathcal{X}}$. Note that this assumption is true if $P_{\mathcal{A}}(\bar{\omega})$ is homogeneous. The cumulative pieces of information $n_{\mathcal{X}}$ read by susceptible individual $u_{\mathcal{X}}$ at time t has a probability

$$\chi_{n_{\mathcal{X}}}^{\mathcal{X}}(k_{\mathcal{X}}, t) = \binom{k_{\mathcal{X}}}{n_{\mathcal{X}}} [\theta_{\mathcal{X}}(t - \varpi_{\mathcal{X}})]^{k_{\mathcal{X}} - n_{\mathcal{X}}} [1 - \theta_{\mathcal{X}}(t - \varpi_{\mathcal{X}})]^{n_{\mathcal{X}}}. \quad (4)$$

At time t , an individual u with degree $\vec{K} = (k_{\mathcal{A}}, k_{\mathcal{B}})$ has not adopted the behavior by time t , i.e., the cumulative pieces of information accessed in both subnetworks \mathcal{A} and \mathcal{B} are less than the adoption thresholds $T_{\mathcal{A}}$ and $T_{\mathcal{B}}$, respectively. At time t , if individual u is active in subnetwork \mathcal{A} he will remain susceptible with a probability

$$F_{\mathcal{A}}(\vec{K}, t) = \sum_{m_{\mathcal{A}}=0}^{k_{\mathcal{A}}} \sum_{n_{\mathcal{B}}=0}^{k_{\mathcal{B}}} \phi_{m_{\mathcal{A}}}^{\mathcal{A}}(k_{\mathcal{A}}, t) \chi_{n_{\mathcal{B}}}^{\mathcal{B}}(k_{\mathcal{B}}, t) \prod_{j_{\mathcal{A}}=0}^{m_{\mathcal{A}}} \prod_{j_{\mathcal{B}}=0}^{n_{\mathcal{B}}} [1 - \pi(j_{\mathcal{A}}, j_{\mathcal{B}})]. \quad (5)$$

Similarly, if individual u is active in subnetwork \mathcal{B} at time t he remains susceptible with a probability

$$F_{\mathcal{B}}(\vec{K}, t) = \sum_{n_{\mathcal{A}}=0}^{k_{\mathcal{A}}} \sum_{m_{\mathcal{B}}=0}^{k_{\mathcal{B}}} \chi_{n_{\mathcal{A}}}^{\mathcal{A}}(k_{\mathcal{A}}, t) \phi_{m_{\mathcal{B}}}^{\mathcal{B}}(k_{\mathcal{B}}, t) \prod_{j_{\mathcal{A}}=0}^{n_{\mathcal{A}}} \prod_{j_{\mathcal{B}}=0}^{m_{\mathcal{B}}} [1 - \pi(j_{\mathcal{A}}, j_{\mathcal{B}})]. \quad (6)$$

The probability of individual u being susceptible is

$$s(\vec{K}, t) = (1 - \rho_0)[p_{\mathcal{A}}F_{\mathcal{A}}(\vec{K}, t) + p_{\mathcal{B}}F_{\mathcal{B}}(\vec{K}, t)], \quad (7)$$

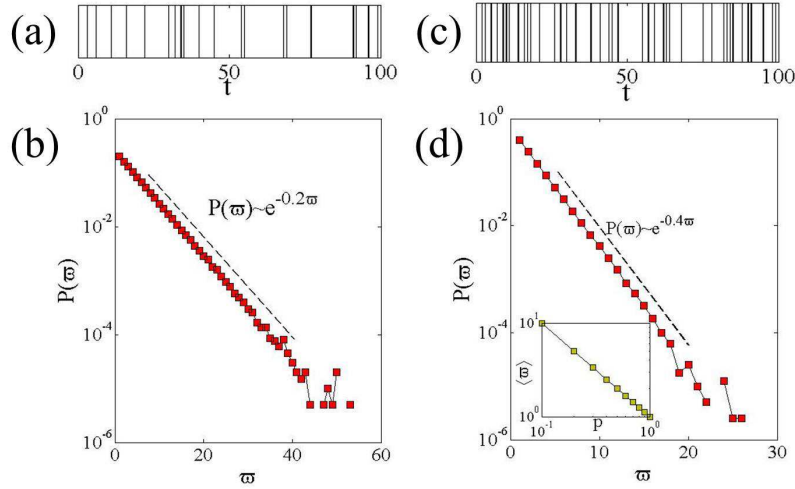


Figure 2. (Color online) Dynamics of social contagions on RR-RR multiplex networks. Active events in subnetwork \mathcal{A} , i.e., individuals are active in subnetwork \mathcal{A} , versus time ϖ with (a) $p = 0.8$ and (c) $p = 0.6$, respectively. The time interval distribution $P(\varpi)$ between two consecutive actives in subnetwork \mathcal{A} with (b) $p = 0.8$ and (d) $p = 0.6$, respectively. We set other parameters to be $\rho_0 = 0.1$, $\gamma = 1.0$, $k = 10$, $\lambda_{\mathcal{A}} = \lambda_{\mathcal{B}} = 0.9$, and $T_{\mathcal{A}} = T_{\mathcal{B}} = 3$.

where $1 - \rho_0$ indicates that an individual is initially susceptible, and $p_{\mathcal{X}} = \frac{1}{N} \sum_{u=1}^N p_u^{\mathcal{X}}$ is the average probability that an individual is active in subnetwork \mathcal{X} . Note that $p_{\mathcal{A}} = 1 - p_{\mathcal{B}}$. Considering the degree distribution $P(\vec{K})$, the fraction of susceptible individuals at time t is

$$S(t) = \sum_{\vec{K}} P(\vec{K}) s(\vec{K}, t). \quad (8)$$

A neighbor $v_{\mathcal{X}}$ of individual $u_{\mathcal{X}}$ in subnetwork \mathcal{X} can be susceptible, adopted, or recovered, thus $\theta_{\mathcal{X}}(t)$ can be divided into

$$\theta_{\mathcal{X}}(t) = \xi_S^{\mathcal{X}}(t) + \xi_A^{\mathcal{X}}(t) + \xi_R^{\mathcal{X}}(t), \quad (9)$$

in which $\xi_S^{\mathcal{X}}(t)$ [$\xi_A^{\mathcal{X}}(t)$ or $\xi_R^{\mathcal{X}}(t)$] is the probability that individual $v_{\mathcal{X}}$ is susceptible (adopted or recovered) and has not transmitted the information to $u_{\mathcal{X}}$ by time t .

If individual $u_{\mathcal{X}}$ is initially susceptible he cannot transmit the information to their susceptible neighbors $v_{\mathcal{X}}$ in subnetworks \mathcal{X} because the individual is in the cavity state. When individual $v_{\mathcal{X}}$ with degree $k'_{\mathcal{X}}$ is susceptible, he also cannot transmit information to $u_{\mathcal{X}}$. At time t , if individual $v_{\mathcal{X}}$ is active in subnetwork \mathcal{X} the probability that he reads $m_{\mathcal{X}}$ pieces of information from this subnetwork is

$$\tau_{m_{\mathcal{X}}}^{\mathcal{X}}(k'_{\mathcal{X}}, t) = \binom{k'_{\mathcal{X}} - 1}{m_{\mathcal{X}}} \theta_{\mathcal{X}}(t)^{k'_{\mathcal{X}} - m_{\mathcal{X}} - 1} [1 - \theta_{\mathcal{X}}(t)]^{m_{\mathcal{X}}}. \quad (10)$$

In contrast, individual v can only read the information at time $t - \varpi_{\mathcal{X}}$ in subnetwork \mathcal{X} when he is active in subnetwork \mathcal{Y} at time t . Similar to that in Eq. (4), the probability that individual $v_{\mathcal{X}}$ reads $n_{\mathcal{X}}$ pieces of information is

$$\varsigma_{n_{\mathcal{X}}}^{\mathcal{X}}(k'_{\mathcal{X}}, t) = \binom{k'_{\mathcal{X}} - 1}{n_{\mathcal{X}}} \theta_{\mathcal{X}}(t - \varpi_{\mathcal{X}})^{k'_{\mathcal{X}} - n_{\mathcal{X}} - 1} [1 - \theta_{\mathcal{X}}(t - \varpi_{\mathcal{X}})]^{n_{\mathcal{X}}}. \quad (11)$$

Individual $v_{\mathcal{X}}$ remains susceptible when the cumulative pieces of information he has read from neighbors in subnetwork \mathcal{X} is lower than their adoption threshold $T_{\mathcal{X}}$ in the absence of individual $u_{\mathcal{X}}$. When v is active in subnetwork \mathcal{X} , he reads $n_{\mathcal{Y}}$ pieces of information in subnetwork \mathcal{Y} with a probability $\chi_{n_{\mathcal{Y}}}^{\mathcal{Y}}(k'_{\mathcal{Y}}, t)$ [see Eq. (4)]. Thus the probability that individual v is susceptible is

$$\Psi_{\mathcal{X}}^{\mathcal{X}}(\vec{K}, t) = \sum_{m'_{\mathcal{X}}=0}^{k'_{\mathcal{X}}-1} \sum_{n'_{\mathcal{Y}}=0}^{k'_{\mathcal{Y}}} \tau_{m'_{\mathcal{X}}}^{\mathcal{X}}(k'_{\mathcal{X}}, t) \chi_{n'_{\mathcal{Y}}}^{\mathcal{Y}}(k'_{\mathcal{Y}}, t) \prod_{j'_{\mathcal{X}}=0}^{m'_{\mathcal{X}}} \prod_{j'_{\mathcal{Y}}=0}^{n'_{\mathcal{Y}}} [1 - \pi(j'_{\mathcal{X}}, j'_{\mathcal{Y}})]. \quad (12)$$

Similarly, when individual v is active in subnetwork \mathcal{Y} the probability that v will read $n_{\mathcal{X}}$ and $m_{\mathcal{Y}}$ pieces of information from subnetworks \mathcal{X} and \mathcal{Y} is $\varsigma_{n_{\mathcal{X}}}^{\mathcal{X}}(k'_{\mathcal{X}}, t)$ and $\phi_{m_{\mathcal{Y}}}^{\mathcal{Y}}(k'_{\mathcal{Y}}, t)$, respectively. The probability that individual v is susceptible is

$$\Psi_{\mathcal{X}}^{\mathcal{Y}}(\vec{K}, t) = \sum_{n'_{\mathcal{X}}=0}^{k'_{\mathcal{X}}-1} \sum_{m'_{\mathcal{Y}}=0}^{k'_{\mathcal{Y}}} \varsigma_{n'_{\mathcal{X}}}^{\mathcal{X}}(k'_{\mathcal{X}}, t) \phi_{m'_{\mathcal{Y}}}^{\mathcal{Y}}(k'_{\mathcal{Y}}, t) \prod_{j'_{\mathcal{X}}=0}^{n'_{\mathcal{X}}} \prod_{j'_{\mathcal{Y}}=0}^{m'_{\mathcal{Y}}} [1 - \pi(j'_{\mathcal{X}}, j'_{\mathcal{Y}})]. \quad (13)$$

When an initially susceptible individual v is active in subnetwork \mathcal{X} , the probability that he remains susceptible is

$$\Theta_{\mathcal{X}}(\vec{K}, t) = p_{\mathcal{X}} \Psi_{\mathcal{X}}^{\mathcal{X}}(\vec{K}, t) + p_{\mathcal{Y}} \Psi_{\mathcal{X}}^{\mathcal{Y}}(\vec{K}, t). \quad (14)$$

In an uncorrelated network, individual u connects to individual v with a degree $k'_{\mathcal{X}}$ in subnetwork \mathcal{X} with a probability $k'_{\mathcal{X}} P(\vec{K}) \Theta_{\mathcal{X}}(\vec{K}, t) / \langle k_{\mathcal{X}} \rangle$, where $\langle k_{\mathcal{X}} \rangle$ is the average degree of subnetwork \mathcal{X} . Thus the probability that individual $u_{\mathcal{X}}$ connects to a susceptible individual in subnetwork \mathcal{X} is

$$\xi_S^{\mathcal{X}}(t) = (1 - \rho_0) \frac{1}{\langle k_{\mathcal{X}} \rangle} \sum_{\vec{K}} k'_{\mathcal{X}} P(\vec{K}) \Theta_{\mathcal{X}}(\vec{K}, t). \quad (15)$$

If the information transmits through an edge at time t in subnetwork \mathcal{X} , the edge will not fulfill the definition of $\theta_{\mathcal{X}}(t)$. The decreasing of $\theta_{\mathcal{X}}(t)$ is thus

$$\frac{d\theta_{\mathcal{X}}(t)}{dt} = -p_{\mathcal{X}} \lambda_{\mathcal{X}} \xi_A^{\mathcal{X}}(t). \quad (16)$$

For $\xi_R^{\mathcal{X}}(t)$ to grow, (i) the information cannot be transmitted through the edge and (ii) the adopted individual must recover at time t . The evolution of $\xi_R^{\mathcal{X}}(t)$ is

$$\frac{d\xi_R^{\mathcal{X}}(t)}{dt} = \gamma(1 - p_{\mathcal{X}} \lambda_{\mathcal{X}}) \xi_A^{\mathcal{X}}(t). \quad (17)$$

Combining Eqs. (16) and (17), and the initial condition $\theta_{\mathcal{X}}(0) = 1$ and $\xi_R^{\mathcal{X}}(0) = 0$, gives us

$$\xi_R^{\mathcal{X}}(t) = \frac{\gamma(1 - p_{\mathcal{X}} \lambda_{\mathcal{X}})[1 - \theta_{\mathcal{X}}(t)]}{p_{\mathcal{X}} \lambda_{\mathcal{X}}}. \quad (18)$$

We use Eqs. (9), (15), (16), and (18) to obtain the value of $\theta_{\mathcal{X}}(t)$.

Using the evolution process of the behavior spreading dynamics described in Sec. 2, we get the evolution equations of the fraction of individuals in the adopted and recovered states,

$$\frac{dA(t)}{dt} = -\frac{dS(t)}{dt} - \gamma A(t), \quad (19)$$

and

$$\frac{dR(t)}{dt} = \gamma A(t), \quad (20)$$

respectively. Combining Eqs. (8) and (19)–(20), we obtain the time evolution of the behavior spreading dynamics in multiplex networks. When $t \rightarrow \infty$, the final behavior adoption size is denoted $R(\infty)$.

We next examine the growth pattern of the final behavior adoption size $R(\infty)$ versus the information transmission probability $\vec{\lambda} = (\lambda_{\mathcal{A}}, \lambda_{\mathcal{B}})$ and the CCA probability p . We first study the effects of the time-delays induced by CCA characteristic on the dynamics of social contagions by investigating another social contagion model without time-delays, in which assumes that a susceptible individual becomes adopted once his received accumulated pieces of information is equal or larger than the adoption threshold in any subnetwork. Figure 3(a) shows the time-delay induced by CCA characteristic affects behavior spreading, including the time evolutions of susceptible $S(t)$, adopted $A(t)$, and recovered $R(t)$ individuals. We find that $S(t)$ [$R(t)$] decreases [increases] with t , and that $A(t)$ first increases and then decreases. Note that the time-delay induced by CCA slows the behavior adoption. To quantify the slow-down caused by CCA, we compute the stabilizing time of the system t_{\max} , i.e., the average time needed for the system to reach the final state. When $0 \leq p \leq 0.5$, we find that t_{\max} first increases with p and then decreases. When the p value is small, most individuals are active in subnetwork \mathcal{B} . When susceptible individuals receive information that exceeds their adoption threshold, they adopt the behavior. When the p value is increased, some individuals become active in subnetwork \mathcal{A} but must wait for a long period of time before adopting the behavior when their received information is larger than their adoption threshold. Thus t_{\max} first increases. When the p value is large, fewer individuals adopt the behavior (see Fig. 4) and t_{\max} thus decreases. The inset of Fig. 3(b) shows retardation time Δt_{\max} for social contagion models with and without time-delays. Note that Δt_{\max} first increases with p and then decreases. We find the same phenomena when $0.5 \leq p \leq 1.0$ because subnetworks \mathcal{A} and \mathcal{B} are both RR networks.

Figure 3(a) shows that the time-delays induced by CCA characteristic do not affect the final behavior adoption size $R(\infty)$. This is because when a susceptible individual fulfills the behavior adoption conditions, the time-delays only affect the behavior adoption time. This also indicates that the critical points of the system remain the same when there are no time-delays in behavior adoption, i.e., a susceptible individual adopts the new behavior as soon as the received pieces of information exceed or equal the adoption threshold and regardless of which subnetwork he is currently active in. Thus in examining the final state of the behavior, we disregard time-delays, i.e., Eqs. (4) and (11) are the same as Eqs. (2) and (10), respectively.

In the final state, i.e., when $t \rightarrow \infty$, we have $d\theta_{\mathcal{X}}(t)/dt = 0$ and $\theta_{\mathcal{X}}(t) = \theta_{\mathcal{X}}(t - \varpi_{\mathcal{X}}) = \theta_{\mathcal{X}}^*$. Combining Eqs. (9), (15)–(16), and (18), we obtain

$$\begin{aligned} \theta_{\mathcal{X}}^* &= (1 - \rho_0) \frac{\sum_{\vec{K}} k_{\mathcal{X}} P(\vec{K}) \Theta_{\mathcal{X}}(\vec{K}, \infty)}{\langle k_{\mathcal{X}} \rangle} + \frac{\gamma(1 - p_{\mathcal{X}} \lambda_{\mathcal{X}})[1 - \theta_{\mathcal{X}}^*]}{p_{\mathcal{X}} \lambda_{\mathcal{X}}} \\ &= f_{\mathcal{X}}(\theta_{\mathcal{A}}^*, \theta_{\mathcal{B}}^*). \end{aligned} \quad (21)$$

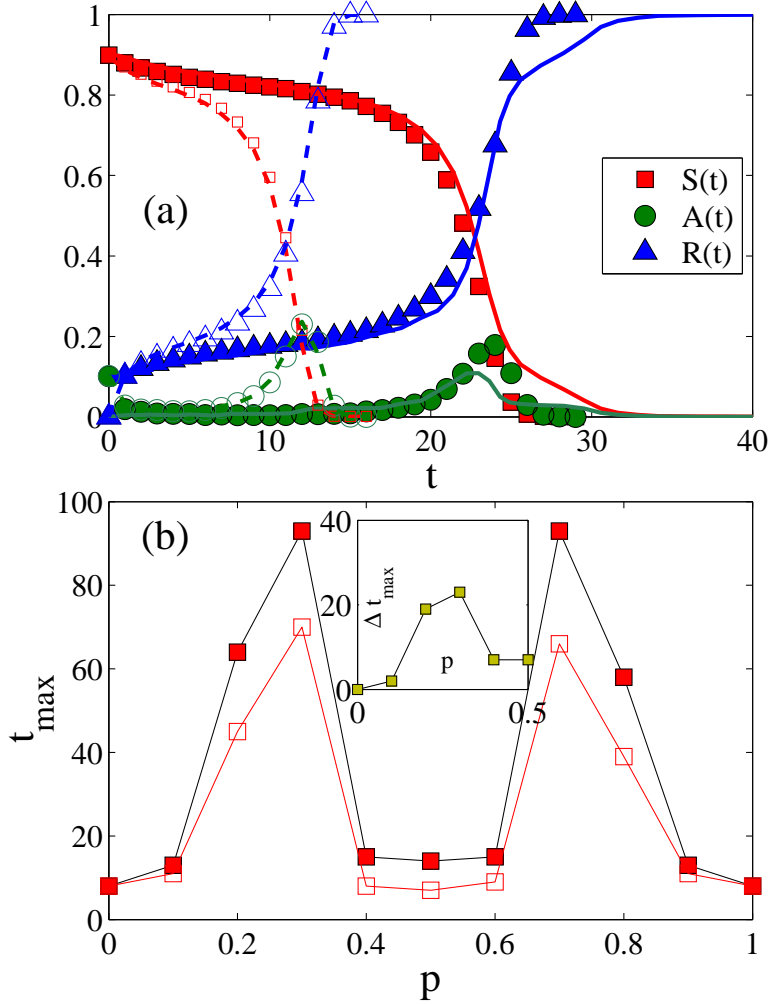


Figure 3. (Color online) Dynamics of social contagions on RR-RR multiplex networks. (a) The time evolutions of susceptible $S(t)$, adopted $A(t)$ and recovered $R(t)$ individuals with (solid symbols) and without (empty symbols) time-delays when $p = 0.8$. The symbols are numerical simulation results and lines are the theoretical predictions. (b) The stabilizing time of the system t_{\max} with (solid symbols) and without (empty symbols) time-delays versus p . The inset of (b) shows the retardation time as a function of p for the system with or without time-delays. We set other parameters to be $\rho_0 = 0.1$, $\gamma = 1.0$, $k = 10$, $\lambda_A = \lambda_B = 0.9$, and $T_A = T_B = 3$.

When $\rho_0 \rightarrow 0$, then $\theta_{\chi}^* = 1$ is a trivial solution of Eq. (21), but this vanishingly small fraction of seeds cannot trigger global behavior adoption because $T_{\chi} > 1$ [33]. To stimulate global behavior adoption, we need a finite fraction of individuals as seeds. Here $\theta_{\chi}^* = 1$ is no longer the solution of Eq. (21), which now has one or three nontrivial solutions (including multiplicity), which means that a saddle-node bifurcation has occurred [46]. There are two stable fixed solutions, but only the maximum solution is physically meaningful since the individuals in the adopted state persistently transmit the information to their neighbors and

$\theta_{\mathcal{X}}^*$ decreases from unity. If Eq. (21) has only one solution, then $\theta_{\mathcal{X}}^*$ decreases continuously with $\lambda_{\mathcal{X}}$ and this leads to a continuous growth pattern in the final behavior adoption $R(\infty)$. If the number of solutions of Eq. (21) vary with the dynamical parameters, then the growth pattern of $R(\infty)$ will be discontinuous, because a meaningful solution decreases abruptly at such critical conditions as the critical information transmission probability $\vec{\lambda}_c$ and the critical CCA probability p_c . The discontinuous critical points of $\vec{\lambda}_c$ and p_c can be obtained by solving both Eq. (21) and

$$\frac{\partial f_{\mathcal{A}}(\theta_{\mathcal{A}}^*, \theta_{\mathcal{B}}^*)}{\partial \theta_{\mathcal{B}}^*} \frac{\partial f_{\mathcal{B}}(\theta_{\mathcal{A}}^*, \theta_{\mathcal{B}}^*)}{\partial \theta_{\mathcal{A}}^*} = 1. \quad (22)$$

In other words, the curves of $f_{\mathcal{A}}(\theta_{\mathcal{A}}^*, \theta_{\mathcal{B}}^*)$ and $f_{\mathcal{B}}(\theta_{\mathcal{A}}^*, \theta_{\mathcal{B}}^*)$ are tangent to each other at the discontinuous critical point [47, 48].

4. Numerical simulations

Here we perform extensive simulations on multiplex networks, including RR-RR networks [i.e., in which each subnetwork is a randomly regular (RR) network] and ER-SF networks [i.e., in which subnetworks \mathcal{A} and \mathcal{B} are Erdős-Rényi (ER) [49] and scale-free (SF) [32] networks, respectively]. In each case we set the network size, average degree, and recovery probability to be $N = 10^4$, $\langle k_{\mathcal{A}} \rangle = \langle k_{\mathcal{B}} \rangle = 10$, and $\gamma = 1.0$, respectively, unless stated otherwise.

4.1. RR-RR multiplex networks

We first study social contagions on RR-RR multiplex networks, in which each node in each subnetwork has a degree $k = 10$. Figure 4(a) shows $R(\infty)$ as a function of λ under different CCA probabilities p . We find that $R(\infty)$ grows with λ *discontinuously* regardless of p . We can understand the discontinuous increasing of $R(\infty)$ by studying the fraction of individuals $g(\infty)$ in the subcritical state. When an individual is in the subcritical state they have received the information but have not adopted the behavior, and the number of information units from distinct neighbors is precisely one less than the adoption threshold in subnetwork \mathcal{A} or \mathcal{B} [33]. Slightly increasing the value of λ can increase the number of subcritical state individuals with information pieces equal to or greater than their threshold [see Fig. 4(b)] and lead to a discontinuous jump in $R(\infty)$. In addition, $R(\infty)$ decreases with p , since an increasing number of susceptible individuals are unable to fulfill the behavior adoption condition. We locate the numerical critical point λ_c^I by studying the number of iterations (NOI) needed to reach the final state, and we take into account only iterations at which at least one individual adopts the behavior. Figure 4(c) shows that at the critical point the NOI values exhibit a peak. Note that our theory accurately predicts $R(\infty)$ and the growth pattern of $R(\infty)$. The deviations around the critical points are caused by the finite-size networks effects [see Fig. 4(a)].

Figures 4(d)–(f) show the affect of p on social contagions. Figure 4(d) shows that the final behavior adoption size $R(\infty)$ versus p is non-monotonic. Specifically, for relatively small values of $\lambda = 0.6$ few susceptible individuals adopt the behavior, and $R(\infty)$ first decreases

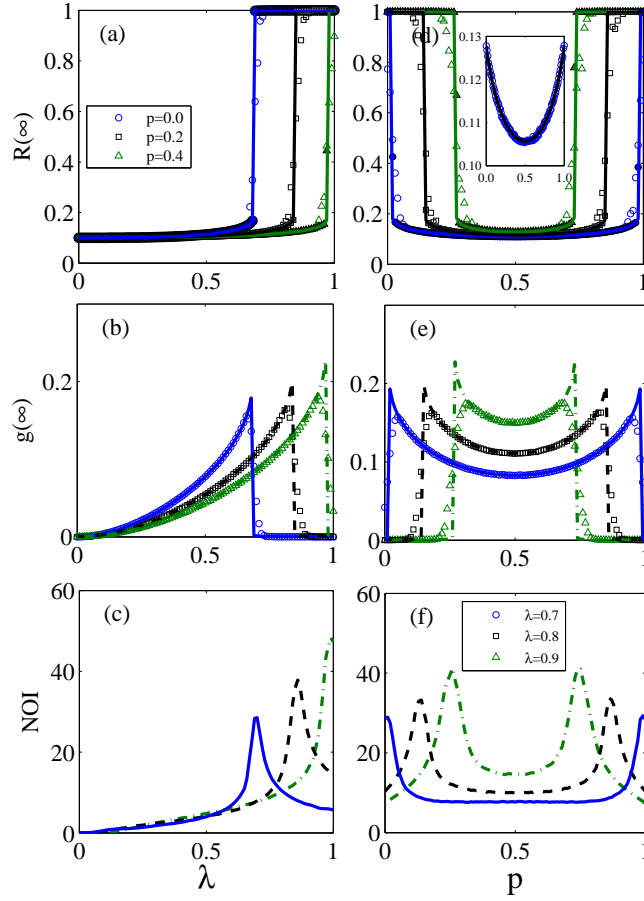


Figure 4. (Color online) Behavior spreading on RR-RR networks. (a) Final behavior adoption size $R(\infty)$, (b) NOI and (c) the fraction of individuals in the subcritical state $g(\infty)$ versus information transmission probability λ for CCA probability $p = 0.0, 0.2$ and 0.4 . (d) $R(\infty)$, (e) NOI and (f) $g(\infty)$ versus p for $\lambda = 0.7, 0.8$ and 0.9 . The inset of (d) shows $R(\infty)$ versus p for $\lambda = 0.6$. The empty (full) symbols are the simulated values of $R(\infty)$ at network size $N = 10^4$ ($N = 10^6$). The lines in (a), (b), (d) and (e) are the theoretical values, and are numerical simulation results in (c) and (f). Other parameters are $\rho_0 = 0.1$, $\gamma = 1.0$ and $\langle k \rangle = 10$, respectively.

continuously with p and then increases *continuously* [see the inset in Fig. 4(d)]. For large values of $\lambda = 0.7, 0.8, 0.9$, $R(\infty)$ first decreases *discontinuously* with p and then increases *discontinuously* [see Fig. 4(d)]. We can similarly understand the growth pattern of $R(\infty)$ by studying $g(\infty)$. For a small value of p , e.g., $p = 0.1$ when $\lambda = 0.9$, most individuals in subnetwork \mathcal{A} are active, many individuals adopt the behavior, and few individuals remain in the subcritical state [see Fig. 4(e)]. With the increase of p , fewer individuals are active in subnetwork \mathcal{B} , many individuals in subnetwork \mathcal{A} are in the subcritical state [see Fig. 4(e)], and there is a sharp decrease in $R(\infty)$. By further increasing p , many individuals “jump” between subnetworks \mathcal{A} and \mathcal{B} , and fewer individuals receive one fewer information units than the adoption threshold in the two subnetworks. Thus $g(\infty)$ decreases [see Fig. 4(e)].

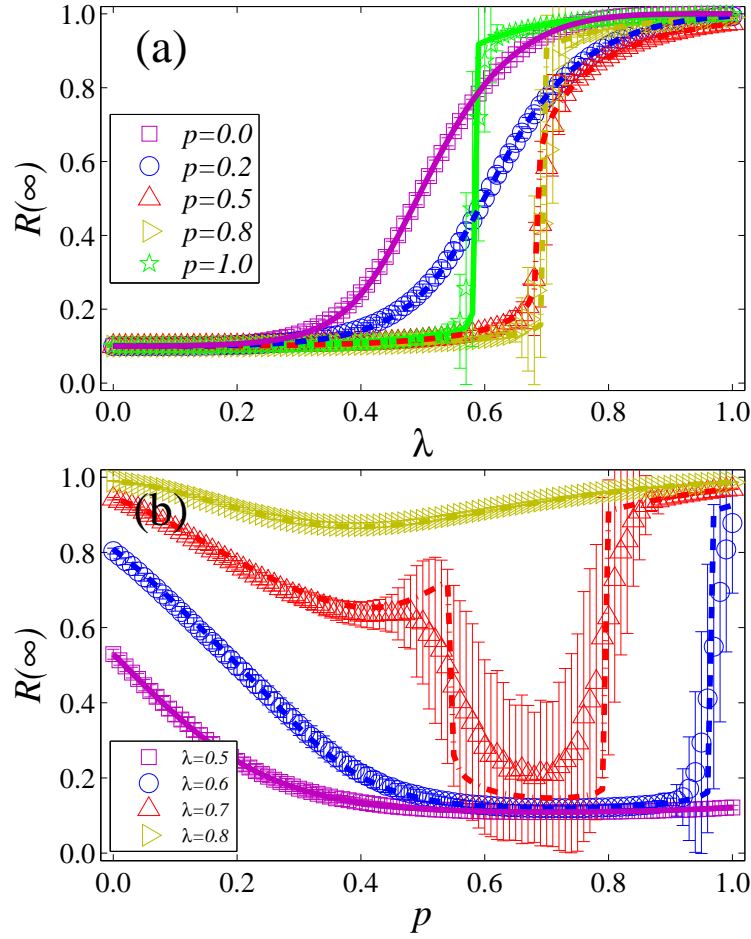


Figure 5. (Color online) Dynamics of social contagions on uncorrelated ER-SF multiplex networks. (a) The final behavior adoption size $R(\infty)$ versus information transmission probability λ under different communication channels alternation probability p . (b) $R(\infty)$ as a function of p for different λ . Lines are the theoretical predictions from Eqs. (7) and (16)-(18). The error bars indicate the standard deviations. Other parameters are set to be $\langle k_A \rangle = 10$, $\langle k_B \rangle = 10$ and $v_B = 3.0$.

Similarly $g(\infty)$ first increases and then decreases discontinuously when the value of p is large. Note that NOI versus p exhibits two peaks at $p_c^1 = 1 - p_c^2$ because the two subnetworks are RR networks [see Fig. 4(f)].

4.2. ER-SF multiplex networks

When studying social contagions on ER-SF multiplex networks, we assume that there are no degree-degree correlations in the intra- and inter-layers. We generate the SF networks using the same method as that used in uncorrelated configuration networks that have a maximum degree $k_{\max} \sim \sqrt{N}$. Figure 5 shows the social contagions on ER-SF networks. Figure 5(a) shows that CCA characteristic changes the growth pattern of $R(\infty)$ versus λ .

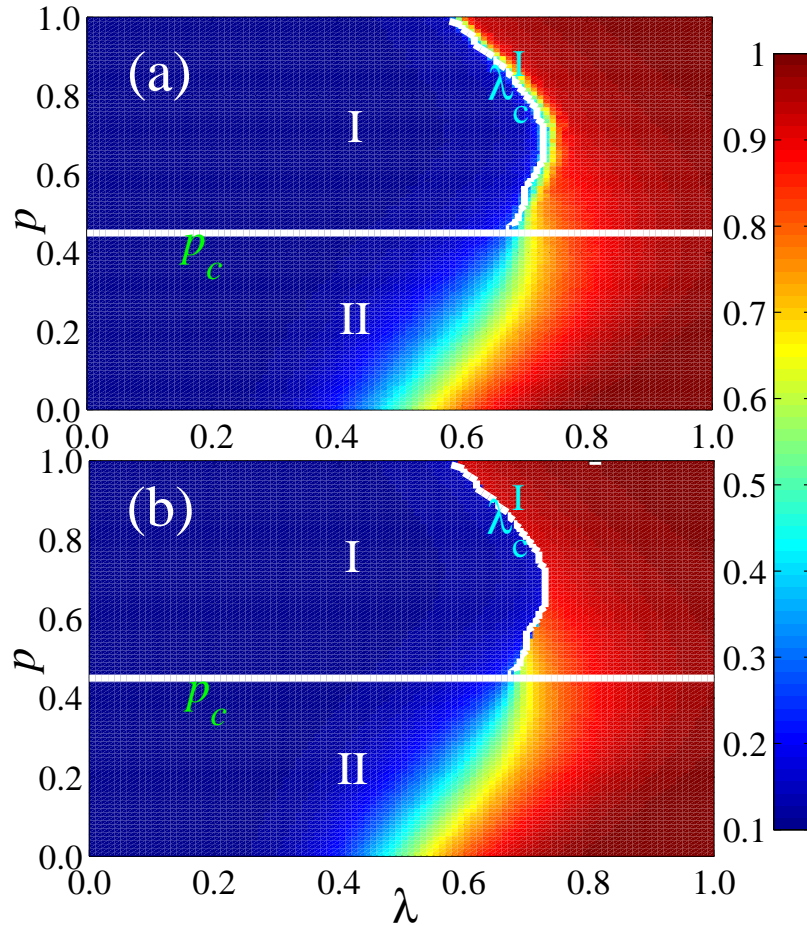


Figure 6. (Color online) Final behavior adoption size $R(\infty)$ versus information transmission probability λ and communication channels alternation probability p on uncorrelated ER-SF networks. Color-coded values of $R(\infty)$ from numerical simulations (a) and theoretical solutions (b) in the parameter plane (λ, p) . The white horizontal line p_c separates the plane into regions I and II. In region I (II), $R(\infty)$ increases discontinuously (continuously) with λ . The white curves denote the theoretical discontinuous critical points λ_c^I . We set other parameters as $\langle k_A \rangle = 10$, $\langle k_B \rangle = 10$ and $v_B = 3.0$.

When $p = 0.0$ (1.0), the number of individuals active only in subnetwork \mathcal{B} (\mathcal{A}) and $R(\infty)$ grow continuously (discontinuously) versus λ (see Ref. [33]). With an increase in p , there is an increasing number of individuals active in the homogeneous subnetwork \mathcal{A} and more individuals are in subcritical state and are more likely to simultaneously adopt the behavior. Thus we see a discontinuous growth in $R(\infty)$.

Figure 5(b) shows that $R(\infty)$ versus p exhibits distinct patterns under different values of λ . For a small value $\lambda = 0.5$, $R(\infty)$ first decreases continuously with p . For a relatively large value, e.g., $\lambda = 0.6$, $R(\infty)$ first decreases continuously with p and then increases discontinuously. Note that when $\lambda = 0.7$, $R(\infty)$ first decreases continuously with p , then increases to a peak at some p , then decreases discontinuously, and finally increases

discontinuously. For a very large value $\lambda = 0.9$, $R(\infty)$ first decreases continuously and then increases continuously. For intermediate values of $0 < p < 1$, the CCA characteristic emerges, which makes individuals' received information in one subnetwork are hard greater than their adoptions, and there is a non-monotonous varying of $R(\infty)$. We can understand the different growth patterns by studying the high degree nodes or hubs, which (i) are more likely to adopt the behavior than those in homogeneous network networks for small values of λ and (ii) lead to individuals adopting the behavior gradually with fewer individuals in the subcritical state simultaneously adopting the behavior [33]. The fraction of hubs in the living subnetwork varies with p . We here define living subnetwork as individuals are active at different time step. For small $\lambda = 0.5$, individuals active in heterogeneous (homogeneous) networks are easily (hardly) adopt the behavior, combining the second role of hubs, $R(\infty)$ thus decreases with p . For relatively larger $\lambda = 0.6$, $R(\infty)$ first decreases continuously since some individuals are active in heterogeneous networks for relatively small p (e.g., $p < 0.5$), and $R(\infty)$ then increases discontinuously because many individuals are active in homogeneous networks and in the subcritical state for large p . The strange phenomena when $\lambda = 0.7$ is also induced by the living network. When p around 0.4, many individuals are active in homogeneous subnetwork \mathcal{A} , $R(\infty)$ thus increases with p . A further increase of p is a slight perturbation that moves many individuals into the subcritical state, and $R(\infty)$ decreases discontinuously. When $\lambda = 0.8$, most individuals adopt the behavior, few individuals are in the subcritical state, and there is only a non-monotonous varying of $R(\infty)$ versus p . We can predict this stated phenomena using our theory. Note that the deviations near the discontinuous points can be eliminated by enlarging network size N .

Figure 6 shows $R(\infty)$ versus the $\lambda-p$ plane. Using the growth pattern of $R(\infty)$ versus λ , we divide the plane into regions I and II according to a critical CCA probability p_c . In region I, $R(\infty)$ grows discontinuously with λ , and in region II, $R(\infty)$ grows continuously with λ . There is thus a crossover phenomenon in the growth pattern: When $p > p_c$, the growth pattern of $R(\infty)$ is discontinuous; otherwise it is continuous. We can explain the growth pattern of $R(\infty)$ using bifurcation theory. The discontinuous critical points λ_c^I exhibit a non-monotonic change with p because of the CCA characteristic. When $p > p_c$, individuals are more likely to be active in subnetwork \mathcal{A} , and thus there are some hubs and many small degree individuals in the living subnetwork. These hubs promote behavior adoption. Increasing p decreases the number of hubs and small degree individuals in the living network, and p_c thus first increases then increases. Our theory agrees well with the numerical simulations.

5. Conclusions

We have systematically investigated how the CCA characteristic affects the dynamics of social contagions. We first proposed a non-Markovian behavior spreading model on multiplex networks in which each individual can only transmit and obtain the information from neighbors in their own subnetwork. To include the CCA characteristic, we assumes that an individual can be active in only one communication layer, and can transmit behavioral information to neighbors and read behavioral information from neighbors within the same

subnetwork at any given time. The CCA characteristic slows an individual's ability to obtain the information from both subnetworks. Thus time-delays in obtaining the information in both subnetworks are introduced. We then perform extensive numerical simulations of artificial multiplex networks and find that the time-delays caused by the CCA characteristic slow-down the behavior adoption process, but do not affect the final behavior adoption size. In addition, the CCA characteristic suppresses the final behavior adoption size $R(\infty)$. We found that CCA changes the growth pattern of $R(\infty)$ versus information transmission probability λ from discontinuous (continuous) to continuous (discontinuous) for ER-SF networks. To quantify the non-Markovian spreading dynamics, we develop an edge-based compartmental theory that produces results that agree with the numerical simulation results.

We have studied how the CCA characteristic—an important spreading mechanism—affects social contagions. We first construct the connections between human dynamics [50, 51, 52] and social contagions on multiplex networks. Individuals accomplishing different tasks using different communication channels do so in patterns that exhibits memory and burst characteristics. Our results here are the first to investigate the effects of human dynamics on social contagions in multiplex networks. Our theory allows us to understand how the CCA characteristic shapes the spreading dynamics, and it can be used to analyze different dynamic processes in multiplex networks. Our work may stimulate more researches on social contagions that takes into consideration both realistic spreading mechanisms and network topologies.

Acknowledgements

This work was partially supported by the National Natural Science Foundation of China under Grant Nos. 11575041, and 61672238, and Program for Innovation Team Building of Mobile Internet and Big Data at Institutions of Higher Education in Chongqing. LAB knowledge the support of UNMdP and PICT 0429/13.

References

- [1] Boccaletti S, Bianconi G, Criado R, Del Genio C I, Gómez-Gardeñes J, Romance M, Sendiña-Nadal I, Wang Z, and Zanin M 2014 Phys. Rep. **544** 1.
- [2] Gao J, Buldyrev S V, Stanley H E, and Havlin S 2012 Nat. Phys. **8** 40.
- [3] D'agostino G, and Scala A *Networks of networks: the last frontier of complexity* (Springer, 2014).
- [4] Kivelä M, Arenas A, Barthelemy M, Gleeson J P, Moreno Y, and Porter M A 2014 Journal of Complex Networks **2** 203.
- [5] Kim J Y, and Goh K-I 2013 Phys. Rev. Lett. **111** 058702.
- [6] Radicchi F 2014 Phys. Rev. X **4** 021014.
- [7] Buldyrev S V, Parshani R, Paul G, Stanley H E, and Havlin S 2010 Nature **464** 1025.
- [8] Cozzo E, Banos R A, Meloni S, and Moreno Y 2013 Phys. Rev. E **88** 050801.
- [9] Saumell-Mendiola A, Serrano M Á, and Boguna M 2012 Phys. Rev. E **86** 026106.
- [10] Zhang X, Boccaletti S, Guan S, and Liu Z 2015 Phys. Rev. Lett. 2015 **114** 038701.
- [11] Xu E H, Wang W, Xu C, Tang M, Do Y, and Hui P 2015 Phys. Rev. E **92** 022812.
- [12] Dickison M, Havlin S, and Stanley H E 2012 Phys. Rev. E **85** 066109.
- [13] Cozzo E, and Moreno Y 2016 arXiv preprint arXiv:1603.08464.

- [14] Porter M A and Gleeson J P, in *Dynamical Systems on Networks* (Springer, 2016)
- [15] Brummitt C D, Lee K-M, and Goh K-I 2012 Phys. Rev. E **85** 045102.
- [16] Min B, and Goh K-I 2014 Phys. Rev. E **89** 040802.
- [17] Yagan O, and Gligor V 2012 Phys. Rev. E **86** 036103.
- [18] Watts D J 2002 Proc. Natl. Acad. Sci. **99** 5766.
- [19] Lee K-M, Brummitt C D, and Goh K-I 2014 Phys. Rev. E **90** 062816.
- [20] Majdandzic A, Braunstein L A, Curme C, Vodenska I, Levy-Carciente S, Stanley H E, and Havlin S 2016 Nat. Com. **7**.
- [21] Majdandzic A, Podobnik B, Buldyrev S V, Kenett D Y, Havlin S, and Stanley H E 2014 Nat. Phys. **10** 34.
- [22] Wang W, Liu Q-H, Cai S-M, Tang M, Braunstein L A, and Stanley H E 2016 Sci. Rep. **6** 29259.
- [23] Wang W, M. Tang, H. Yang, Y. Do, Y.-C. Lai, and G. Lee 2014 Sci. Rep. **4** 5097.
- [24] Liu Q-H, Wang W, Tang M, and Zhang H-F 2016 Sci. Rep. **6** 25617.
- [25] Granell C, Gómez S, and Arenas A 2013 Phys. Rev. Lett. **111** 128701.
- [26] Funk S, Gilad E, Watkins C, and Jansen V A 2009 Proc. Natl. Acad. Sci. **106** 6872.
- [27] Holme P, and Saramäki J 2012 Phys. Rep. **519** 97.
- [28] Haerter J O, Jamtveit B, and Mathiesen J 2012 Phys. Rev. Lett. **109** 168701.
- [29] Min B, Gwak S-H, Lee N, and Goh K-I 2016 Sci. Rep. **6** 21392.
- [30] De Domenico M, Sole-Ribalta A, Gómez S, and Arenas A 2014 Proc. Natl. Acad. Sci. **111** 8351.
- [31] Starnini M, Baronchelli A, and Pastor-Satorras R 2016 arXiv preprint arXiv:1606.06626.
- [32] Catanzaro M, Boguñá M, and Pastor-Satorras R 2005 Phys. Rev. E **71** 027103.
- [33] Wang W, Tang M, Zhang H-F, and Lai Y-C 2015 Phys. Rev. E **92** 012820.
- [34] Wang W, Tang M, Shu P, and Wang Z 2016 New J Phys. **18** 013029.
- [35] Wang W, Shu P, Zhu Y-X, Tang M, and Zhang Y-C Chaos 2015 **25** 103102.
- [36] Haerter J O, Jamtveit B, and Mathiesen J 2012 Phys. Rev. Lett. **109** 168701.
- [37] Holme P, and Saramaki J 2012 Phys. Rep. **519**.
- [38] Schönfisch B, and de Roos A 1999 BioSystems **51** 123.
- [39] Centola D 2011 Science **334** 1269.
- [40] Wang W, Tang M, Zhang H-F, Gao H, Do Y, and Liu Z-H 2014 Phys. Rev. E **90** 042803.
- [41] Miller J C, and Volz E M 2013 PloS One **8** e69162.
- [42] Miller J C 2011 J Math. Bio. **62** 349.
- [43] Wang W, Tang M, Stanley H E, and Braunstein L A 2017 Rep. Prog. Phys. **80** 036603.
- [44] Karrer B, and Newman M E J 2010 Phys. Rev. E **82** 016101.
- [45] Mieghem P V *Performance Analysis of Communications Systems and Networks* (Cambridge University Press, 2014).
- [46] Strogatz S H *Nonlinear Dynamics and Chaos: With Applications to Physics, Biology, Chemistry and Engineering* (Westview, Boulder, 1994).
- [47] Yuan X, Hu Y, Stanley H E, and Havlin S 2016 arXiv preprint arXiv:1605.04217.
- [48] Parshani R, Buldyrev S V, and Havlin S 2010 Phys. Rev. Lett. **105** 048701.
- [49] Erdős P, and Rényi 1959 Publ. Math. **6** 290.
- [50] Barabasi A-L 2005 Nature **435** 207.
- [51] Vazquez A 2005 Phys. Rev. Lett. **95** 248701.
- [52] Brockmann D, Hufnagel L, and Geisel T 2006 Nature **439** 462.